Journal of Power Sources 196 (2011) 6125–6130

Contents lists available at ScienceDirect

Journal of Power Sources

journal homepage: www.elsevier.com/locate/jpowsour

Tungsten carbide as supports for Pt electrocatalysts with improved CO tolerance in methanol oxidation

Guofeng Cui [a], Pei Kang Shen [b,*], Hui Meng [b,*], Jie Zhao [c], Gang Wu [d]

[a] Key Laboratory of Low-carbon Chemistry & Energy Conservation of Guangdong Province, School of Chemistry and Chemical Engineering, Sun Yat-Sen University, Guangzhou 510275, China
[b] State Key Laboratory of Optoelectronic Materials and Technologies, and Key Laboratory of Low-carbon Chemistry & Energy Conservation of Guangdong Province, School of Physics and Engineering, Sun Yat-sen University, Guangzhou 510275, China
[c] School of Mechanical and Automotive Engineering, South China University of Technology, Guangzhou 510640, China
[d] Materials Physics & Applications Division, Los Alamos National Laboratory, Los Alamos, NM 87545, USA

ARTICLE INFO

Article history:
Received 16 February 2011
Received in revised form 17 March 2011
Accepted 23 March 2011
Available online 31 March 2011

Keywords:
Tungsten carbide
Theoretical calculation
CO poisoning
Methanol oxidation
Fuel cells

ABSTRACT

One anti-CO-poisoning Pt–WC/C catalyst for methanol electro-oxidation is prepared in this work, through depositing platinum on tungsten carbide support using an intermittent microwave heating (IMH) method. The catalyst presents an improved methanol oxidation performance evidenced by a negative shift in onset potential, and increase of peak current density, compared with a commercial Pt/C one. CO stripping experiments indicate that the adsorbed CO is able to be oxidized and removed from the Pt–WC/C catalyst more easily, attesting the enhanced capability of anti-poisoning to CO-like species. Theoretical calculation further provides evidence that the surface electronic structure in Pt–WC/C and Pt/C catalysts is likely different. WC supports could lead to much stronger negative electronic property, which is beneficial for avoiding CO adsorption on the Pt–WC/C catalyst. In the mean time, the electron donating effect generated by WC supports also promotes the ability to oxidize the adsorbed CO-like species on catalysts. In good agreement with experimental results, the theoretical calculation proves the anti-CO-poisoning nature of the Pt–WC/C catalyst, and well explains the origin of the improvement in the electrochemical catalytic performance for effectively accelerating the oxidation of CO to CO_2 in methanol oxidation.

1. Introduction

The commercialization of direct methanol fuel cells (DMFCs) greatly relies on the progress on the key catalyst materials. Currently, platinum (Pt) is still the most commonly used catalyst for methanol oxidation in DMFCs. However, Pt can easily be poisoned by intermediates during methanol electrooxidation, most likely adsorbed CO-like species (CO_{ad}) that only can be oxidized to CO_2 at higher potentials (above 0.6 V). In order to improve the CO poisoning tolerance of Pt catalysts, alloying structures were extensively developed to prevent the Pt catalyst from CO poisoning. The most studied and successful candidate is the PtRu catalyst [1,2]. Based on the bi-functional mechanism and the electron donating effect [3–5], CO_{ad} on the surface of Pt can be oxidized at lower potentials due to the promotional effect of Ru, thus improving the reaction rates of methanol oxidation. In addition to Ru, other metals such as Ir [6] and Au [7] also can be alloyed with Pt to improve the anti-poisoning effect. However, generally the alloyed catalysts are not electrochemically stable in fuel cell environment, and the resolved alloy elements will result in dramatically performance loss, because of not only Pt anode degradation itself, but also cathode contamination due to Ru crossover. Thus, it is important to develop Pt catalysts with high CO tolerance and stability though different strategies, rather than alloying.

The addition of WC into Pt can remarkably increase the amount of OH_{ad} at the Pt sites, which accelerates CO_{ad} oxidation and removal as CO_2, thereby improving the anti-poisoning ability of Pt catalyst. In the electrochemical environment, WC partially changes to the mixture of W(V/VI) oxides, which would promote the dissociation of H_2O into H^+ and OH^-, and provide OH_{ad} to Pt sites. Also this process could facilitate the proton transfer on Pt due to the possible spill over effect [8]. Similar effects also have been observed with other elements in the same group with W, for example PtMo catalyst is found to have better anti-poisoning ability than that of PtRu [9].

Recently, our group has systematically focused on the synthesis of nanostructured WC, and its synergistic effects in electrocatalytic reactions [10–13]. Pt, Pd, Au, Ag nanoparticles were successfully anchored on WC supports in synthesis of composite catalysts for alcohol oxidation and oxygen reduction. The improved catalytic activities have been observed with these catalysts, but the mech-

* Corresponding authors. Tel.: +86 20 84036736; fax: +86 20 84113369.
E-mail addresses: stsspk@mail.sysu.edu.cn (P.K. Shen), menghui@mail.sysu.edu.cn (H. Meng).

0378-7753/$ – see front matter © 2011 Elsevier B.V. All rights reserved.
doi:10.1016/j.jpowsour.2011.03.042

anism still remains unclear. In previous efforts to explore the promotional role of WC in electrocatalysis, Chen and his co-workers comparatively studied the binding energy of CO with WC, Pt/WC and Pt catalysts [14]. Their results pointed out that CO is able to be oxidized much easier on the surface of WC and Pt/WC, relative to Pt, thereby showing lower onset potentials for CO oxidation on these WC containing catalysts. Using the density functional theory (DFT), Shubina and his co-workers also determined the CO adsorption energy and OH binding energy on PtRu, PtMo, PtSn catalysts, and revealed the relevant mechanism for the improved anti-poisoning ability observed with these binary Pt catalyst [15].

In this work, the newly synthesized Pt–WC/C catalyst showed an improved activity in CO and methanol oxidation. CO stripping experiments attests the significantly enhanced CO anti-poisoning ability due to the lower onset potential on the Pt–WC/C catalyst than that of Pt/C catalyst. Importantly, density functional theory (DFT) is applied to study the catalyst electronic structure to provide the origin of the anti-poisoning property derived from WC. A correlation between the electronic structure and the catalytic performance has been established.

2. Experimental

2.1. The preparation of Pt–WC/C catalyst

In a typical procedure to synthesize Pt–WC/C catalyst, 3.7 g ammonium metatungstate (AMT, $(NH_4)_6H_2W_{12}O_{40}{\cdot}xH_2O$)) was first solved in a mixed solution containing 10.0 mL water and 10.0 mL isopropanol. Then 2.5 g Vulcan XC-72R carbon black powder (Cabot corp., USA, S_{BET} = 236.8 $m^2\,g^{-1}$) was added to the above solution followed by a rigorous magnetic stir, and an ultrasonic treatment. After evaporating the solvent from the suspension, the dried powders were heat-treated in a homemade program-controlled microwave oven (2000 W, 2.45 GHz) with a heating procedure of 15 s on and 15 s off for twenty times to obtain WC/C sample as catalyst supports.

Pt–WC/C catalyst was prepared as following. The WC/C powders (200 mg) were dispersed into H_2PtCl_6 solution (18.5 mg mL^{-1}). Then ethylene glycol (EG, 20 mL) was added into the above mixed solution. The solution pH was adjusted to 10 by adding 5 wt% NaOH/EG mixed solution. The mixture was dispersed in an ultrasonic bath for at least 30 min, then heated in the program-controlled microwave oven with a heating procedure of 5 s on and 5 s off for twenty times. After cooling down, the resultant product was filtered, and washed with ultrapure water until no Pt ion was detected. Finally, the catalyst was dried in vacuum oven at 80 °C for 12 h.

2.2. The characterization of the catalysts

Electrochemical measurements were performed on IM6e electrochemical workstation (Zahner-Electrik, Germany). A standard three-electrode cell with separate compartments was used. A Pt foil and saturated calomel electrode (SCE) were used as the counter and reference electrodes, respectively. A glassy carbon disk (0.196 cm^2) deposited with catalyst was used as the working electrode. For working electrode preparation, a catalyst ink was first prepared by dispersing 10 mg of 20 wt% Pt–WC/C powder into 1 mL of ethanol solution containing 5 wt% Nafion (DuPont, USA) (ethanol:Nafion = 20:1). After an ultrasonic stirring, the ink was then deposited on glassy carbon rod, and dried at 80 °C for 30 min. As a reference, Pt/C ink also was prepared by using commercial 50 wt% Pt/C (Columbian Chemicals, Inc., USA) in an identical procedure. In both cases, the total Pt loadings were controlled at 20 μg on disk. The Pt loadings were determined by inductively coupled plasma-atomic emission spectrometry (ICP, IRIS(HR), USA).

The CO stripping experiments were conducted in the following procedures: (i) N_2 was bubbled into the 0.5 M H_2SO_4 solution for 60 min; (ii) CO was bubbled for 30 min while keeping the potential at −0.14 V vs SCE for CO poisoning; (iii) N_2 was bubbled vigorously to remove traces of dissolved CO; (iv) two cyclic voltammetries (CV) were successively performed at a scan rate of 20 mVs^{-1} from −0.14 to 1.0 V vs SCE for the CO oxidation at the first cycle, and from −0.24 V to 1.0 V vs SCE at the second cycle to record the blank CV.

2.3. Theoretical calculation

The calculations were carried out with the Gaussian 03 program [16], using the hybrid Becke exchange and Lee, Yang, and Parr correlation (B3LYP) functional method [17–19]. In the geometry optimization, single-point energy calculation, transition state location, and molecular orbital characteristic analysis, 6-311G(d,p) basis set was used for hydrogen, oxygen, and carbon atoms. In the case of Pt atoms, LAN2DZ basis set with the Hay and Wadt effective core pseudopotential was used. These basis sets have also been used by Psofogiannakis et al. to investigate the methane oxidation mechanism on a Pt (1 1 1) cluster [20,21]. The molecular geometry and vibration frequency of all species were calculated based on the Pt cluster structures. As the Pt metal lattice belongs to the face-centered cubic (fcc) structure, five atoms are in the first layer, and four atoms in the second layer. In all calculations, the metal cluster moieties are assumed to be fixed. For characterization of transition state (TS), the single imaginary frequency is confirmed. The energies of the TS and product are obtained with respect to that of the reactant.

3. Results and discussion

3.1. Comparison of the anti-poisoning ability of Pt/C and Pt–WC/C

CVs of the methanol oxidation on Pt/C and Pt–WC/C catalysts before and after 1000 cycles are compared in Fig. 1a. It can be seen that the Pt–C/WC catalyst is able to generate a nearly two time higher peak current density than Pt/C. Moreover, after 1000 potential cycles in CV, the activities for both catalysts also were recorded to determine their stabilities in methanol oxidation. The results indicate that the peak current density on Pt–WC/C decreased 14.1% after 1000 cycles, which is much stable than traditional Pt/C catalysts with a activity drop of 43.1%. This is indicative of a better stability for Pt–WC/C, when compared to Pt/C. The onset potential of methanol is considered as an important factor to determine the intrinsic activity of catalysts. Fig. 1a also shows that the onset potential of methanol oxidation observed with Pt–WC/C was a negative shift of 92 mV to that of Pt/C. This suggests that the addition of WC into Pt/C effectively reduce the overpotential of methanol oxidation, which would remarkably lead to an improved performance in a direct methanol fuel cell.

The origin of the onset potential shift in the methanol oxidation on Pt–WC/C catalyst was investigated by CO stripping experiment as shown in Fig. 1b. It can be seen that the peak potentials for CO oxidation on Pt–WC/C and Pt/C electrodes are 0.467 V and 0.554 V vs SCE, respectively. The peak potential for CO oxidation on Pt–WC/C catalyst is 87 mV negative than that on Pt/C catalyst. This means that CO is able to be oxidized on Pt–WC/C catalyst at lower potential relative to conventional Pt/C. The presence of WC can enhance the CO-tolerance for the catalyst, which could be advantageous for lowing overpotential in direct alcohol fuel cells for methanol oxidation.

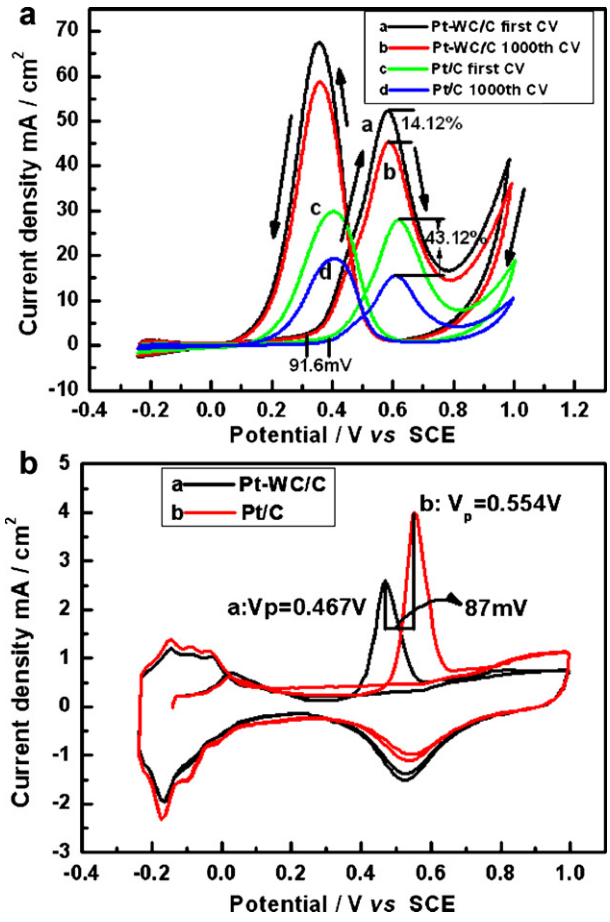

Fig. 1. (a) Methanol oxidation on Pt/C and Pt–WC/C catalysts in 1 mol dm^{-3} methanol + 0.5 mol dm^{-3} H_2SO_4 at 50 mV s^{-1}. a: the first cycle of Pt–WC/C, b: Pt–WC/C after 1000 cycles, c: the first cycle of Pt/C and d: Pt/C after 1000 cycles (b) CO stripping data on Pt/C and Pt/WC in 0.5 mol dm^{-3} H_2SO_4 at scan rate of 20 mV s^{-1}.

3.2. Surface electronic structure

In order to interpret the possible reason of enhanced CO anti-poisoning ability observed with Pt–WC/C catalyst, the structure and surface electrostatic potential are calculated, and shown in Fig. 2. There are two distinct properties for the surface electrostatic potential on the catalyst. First, as shown in Fig. 2(a) and (b), for both Pt and WC, the negative electronic density concentrated on the central atoms is marked with red zones. This indicates that both Pt and W atoms have strong electron donating properties. It is worth noting that the higher electronic density around W cluster implies a stronger electron donating property, when compared to that of Pt atoms. Second, when Pt is deposited onto WC supports, the negative electronic density only found around Pt atoms, no longer on W atoms center anymore. The highest negative electronic intensity calculated from the Pt/WC is $-3.758\,e^{-2}$ that is twice larger than that of Pt, $-1.364\,e^{-2}$. The consequence could be attributable to the electron donating property of WC supports to anchored Pt cluster.

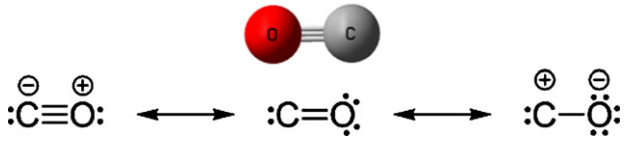

Fig. 3. Atomic structure and electronic model of CO molecule.

Fig. 3 shows the atomic structure and electronic model of CO molecule. The bond length between carbon and oxygen atoms is 112.8 pm, which is consistent with a partial triple bond. Generally, CO molecule can be represented by three resonance structures, among which the leftmost structure is relatively dominant to atomic structure and electronic distribution. Also, atomic formal charge and electronegativity could result in a small bond dipole moment with the negative end on the carbon atom [22,23]. This is due to that the highest occupied molecular orbital has close energy to that of carbon's *p* orbital, even though oxygen atom has a greater electronegativity in CO molecule. As a consequence, higher electron density is found near the carbon atom. In addition, the lower electro-negativity of carbon creates a much more diffuse electron cloud, enhancing the polarizability. Based on above analysis, the chemical adsorption of CO is very likely to occur on the carbon atom, rather than the oxygen atom.

From the point of physical adsorption, CO can be easily absorbed on the catalyst, but hardly desorbs from it. One effective way to avoid CO poisoning is to prevent its absorption on the Pt sites. As the oxygen atom in CO molecule is in an electronic saturation state, the carbon atom can be preferentially absorbed on the catalyst. The carbon atom tends to adsorb on atoms of catalyst with positive electronic state, and then lose electrons in the adsorption process. Usually, CO molecular would preferential adsorb on the Pt sites where located at the edge place. However, in the case of Pt–WC/C catalyst, the electrostatic potential of Pt atom is remark-

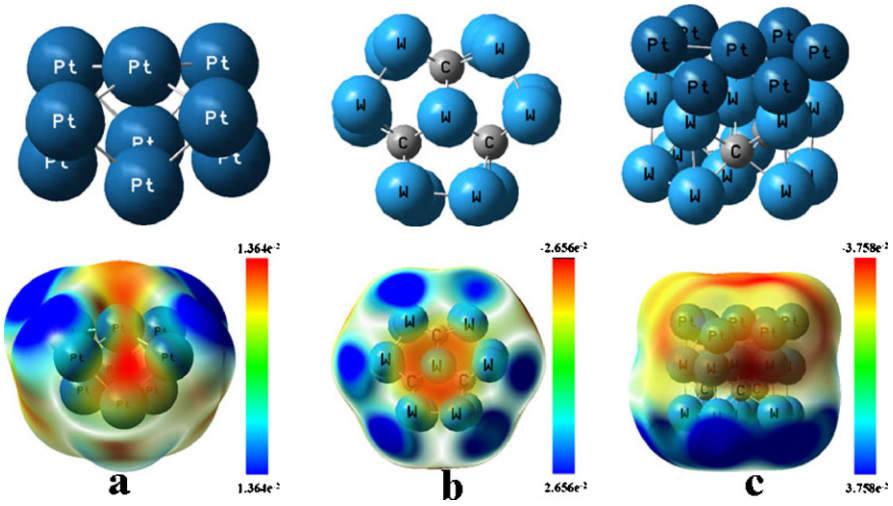

Fig. 2. Structure and surface electrostatic potential of catalyst (a) Pt_9 cluster, (b) WC and (c) Pt_7/WC.

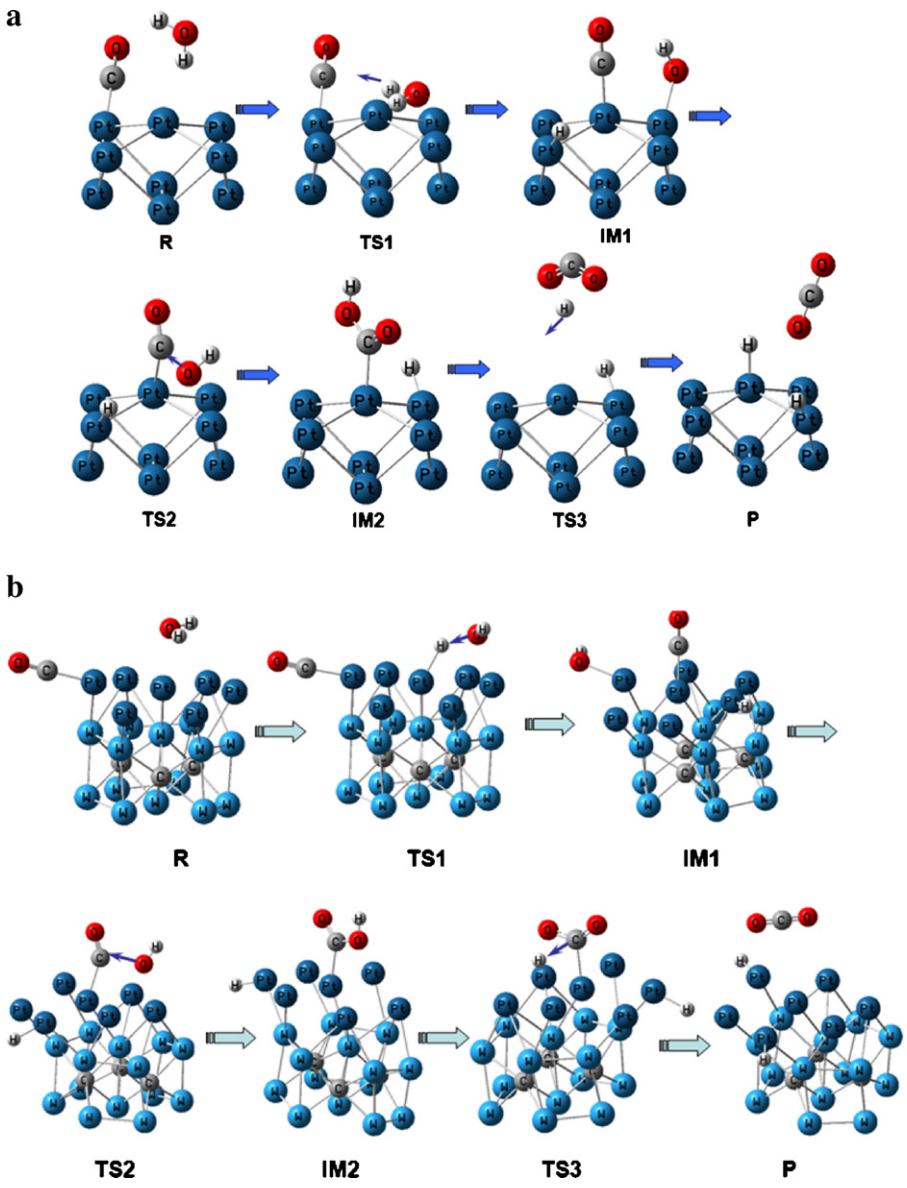

Fig. 4. Geometry optimized of intermediates and transition states on the reaction processes of CO oxidation on Pt_9 (a) and Pt_9/WC (b), obtained at the B3LYP/6-311G(d,p) level for main group element atoms and at the LANL2DZ level for Pt and W. Dark blue, light blue, grey, red and white spheres represent the Pt, W, carbon, oxygen and hydrogen atoms, respectively. The blue arrows represent the vibration mode at the imaginary frequency in the transition state. (For interpretation of the references to color in this sentence, the reader is referred to the web version of the article.)

ably increased due to the electron donating property of WC. As a result, Pt becomes the center of negative electronic density and exhibits negative electronic property, so CO absorption on the Pt sites in Pt–WC/C catalyst is much weaker than that on traditional Pt surface without modification of WC. In brief, the electron donating property derived from WC may enhance the CO anti-poisoning ability for Pt catalyst at a low over-potential condition.

3.3. Oxidation of CO

Promoting the oxidation of CO at low potential is another way to improve Pt catalyst anti-poisoning ability during methanol oxidation. Usually, this process occurs at a high over-potential, as the oxidation of CO needs the participation of OH group formed at high potential to dissociate water molecule. Figs. 4 and 5 demonstrate CO oxidation process on Pt_9 (a) and Pt_9/WC (b) clusters, as well as the corresponding potential energy profiles. The CO oxidation consists of three elemental steps. The first step (R → TS1 → IM1) is the formation of OH• from water decomposition. In this step, an energy barrier of 38.7 kJ mol^{-1} on Pt_9 surface is calculated, which is lower than that on Pt_7/WC surface, suggesting that the Pt surface has higher catalytic activity than WC supports. The formation of OH usually is caused by water molecular broken on two Pt atoms located on surface defects, which have different surface charge. Thus, the defects on Pt surface maybe is very important to help on changing the surface charge, and then possibly improving the catalytic activity [25,26]. The second step (IM1 → TS2 → IM2) is the combination of CO and OH; the third one (IM2 → TS3 → P) is the formation of CO_2. This analysis of transition states on the CO oxidation process as shown in Fig. 4 implies that that the oxidation of CO on Pt and Pt/WC has the same processes.

Fig. 6 shows a comparison of the relative energy in transition states on the Pt–WC/C and Pt/C catalysts. The hydroxide radicals (OH•) were believed as key species in the process of CO oxidation. Thus, the OH was chosen as an oxidizing reactant in this calculation, which is generated either from H_2O molecule decomposition

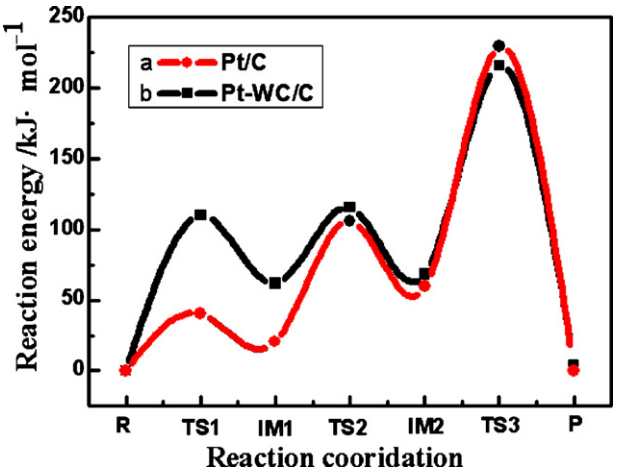

Fig. 5. Potential energy profile of the reaction processes of CO oxidation on Pt_9 (a) and Pt_9/WC (b), obtained at the B3LYP/6-311G(d,p) level for main group element atoms and at the LANL2DZ level for Pt and W.

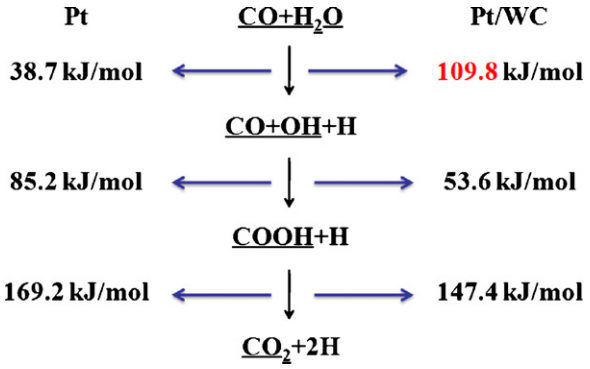

Fig. 6. comparsion of relative energy on transition states for CO oxidation on a Pt/C and Pt–WC/C surface.

in acid condition [21] or from OH by losing one electron in alkaline condition [24]. In this work, in line with our electrochemical measurements in a 0.5 M H_2SO_4 acid solution, water decomposition pathway to produce OH was considered. Based on the calculation in Fig. 6, the energy barrier of water decomposition step on Pt/WC is higher than that on Pt/C. However, in the following two steps of CO/OH combination and CO_2 formation, the energy barrier on Pt_7/WC is much lower than that on Pt_9 surface. The stronger electron donating property of WC could be favorite to oxidize CO into CO_2. The DFT analysis is in a good agreement with the electrochemical measurements as shown in Fig. 1.

Fig. 7 demonstrates the transition state with the highest energy barrier in the CO oxidation process to further explain the higher electro-catalytic activity of Pt–WC/C relative to traditional Pt/C catalyst. In the CO_2 desorbing step, the electrostatic potential for the oxygen atom on Pt_7/WC ($-6.565\,e^{-2}$) is more negative than that on Pt_9 ($-4.384\,e^{-2}$). As a matter of fact, the negative potential would facilitate the removal of CO_2 from the catalyst surface. Thus, the high catalytic activity observed with Pt–WC/C catalyst also is related to the electron donating effect provided by WC supports.

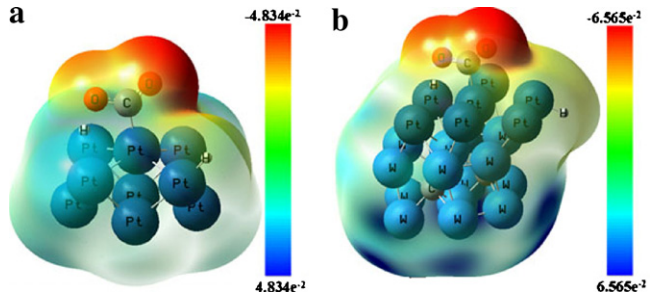

Fig. 7. Surface electrostatic potential of the highest energy barrier transition states (TS3) in CO oxidation mechanism on (a) Pt_9 and (b) on Pt_7/WC.

4. Conclusions

A newly prepared Pt–WC/C electrocatalyst through loading Pt on WC supports exhibits an improved CO anti-poisoning property, when compared to traditional carbon supported Pt catalysts. The surface electrostatic potential calculation indicates that WC supports could provide stronger negative electronic property to Pt atoms in the Pt–WC/C catalysts through an electron donating effect. In the CO adsorbing step, the electron donating effect would be beneficial for avoiding CO adsorption on the Pt catalyst, which occurs in the low overpotential. Also, in the CO oxidation step, the electron donating effect plays a promotional role to enhance the oxidation process, which occurs in the high overpotential. The theory calculations results well explain the observed improvement of CO tolerance on Pt–WC/C catalyst, due to a possible synergistic effect between Pt and WC.

Acknowledgements

The work was financially supported by the National Natural Science Foundation of China (21073241, U1034003), and the China National 863 Program (2009AA05Z110, 2009AA034400). Dr. G.F. Cui is gratefully acknowledge the financial support by National Natural Science Foundation of China (50801070) and Plant Nursery Projects of Guangdong Province (31000-3211602). Dr. H. Meng thanks the New Teacher Funding of Sun Yat-sen University (30000-3126170), and Doctoral Fund of Ministry of Education of China (20100171120022).

References

[1] W. Chrzanowski, A. Wieckowski, Langmuir 13 (1997) 5974–5978.
[2] A. Kowal, M. Li, M. Shao, K. Sasaki, M.B. Vukmirovic1, J. Zhang, N.S. Marinkovic, P. Liu, A.I. Frenkel, R.R. Adzic, Nat. Mater. 8 (2009) 325–330.
[3] T. Yajima, N. Wakabayashi, H. Uchida, M. Watanabe, Chem. Commun. 7 (2003) 828–829.
[4] B. Gurau, R. Viswanathan, R.X. Liu, T. Lafrenz, K. Ley, E. Smotkin, E. Reddington, A. Sapienza, B. Chan, T. Mallouk, S. Sarangapani, J. Phys. Chem. B 102 (49) (1998) 9997–10003.
[5] T. Frelink, W. Visscher, J.A.R. van Veen, Surf. Sci. 335 (1995) 353–360.
[6] C.C. Shan, D.S. Tsai, Y.-S. Huang, S.-H. Jian, C.L. Cheng, Chem. Mater. 19 (2007) 424–431.
[7] G. Selvarani, S. Vinod Selvaganesh, S. Krishnamurthy, G.V.M. Kiruthika, P. Sridhar, S. Pitchumani, A.K. Shukla, J. Phys. Chem. C 113 (2009) 7461–7468.
[8] P.K. Shen, A.C.C. Tseung, J. Electrochem. Soc. 141 (1994) 3082–3086.
[9] L. Li, B.Q. Xu, Acta Phys. Chim. Sin. 21 (10) (2005) 1132–1137.
[10] H. Meng, P.K. Shen, J. Phys. Chem. B 109 (48) (2005) 22705–22709.
[11] H. Meng, P.K. Shen, Chem. Commun. 35 (2005) 4408–4410.
[12] Z.Y. Hu, M. Wu, Z.D. Wei, S.Q. Song, P.K. Shen, J. Power Sources 166 (2) (2007) 458–461.
[13] Z. Zhao, X. Fang, Y. Li, Y. Wang, P.K. Shen, F. Xie, X. Zhang, Electrochem. Commun. 11 (2009) 290–293.
[14] Z.J. Mellinger, E.C. Weigert, A.L. Stottlemyer, J.G. Chen, Electrochem. Solid State Lett. 11 (5) (2008) B63–B67.
[15] T.E. Shubina, M.T.M. Koper, Electrochim. Acta 47 (22–23) (2002) 3621–3628.
[16] M.J. Frisch, G.W. Trucks, H.B. Schlegel, G.E. Scuseria, M.A. Robb, J.R. Cheeseman, J.A. Montgomery Jr., T. Vreven, K.N. Kudin, J.C. Burant, J.M. Millam, S.S. Iyengar, J. Tomasi, V. Barone, B. Mennucci, M. Cossi, G. Scalmani, N. Rega, G.A. Petersson, H. Nakatsuji, M. Hada, M. Ehara, K. Toyota, R. Fukuda, J. Hasegawa, M. Ishida, T. Nakajima, Y. Honda, O. Kitao, H. Nakai, M. Klene, X. Li, J.E. Knox, H.P. Hratchian, J.B. Cross, C. Adamo, J. Jaramillo, R. Gomperts, R.E. Stratmann, O. Yazyev, A.J. Austin, R. Cammi, C. Pomelli, J.W. Ochterski, P.Y. Ayala, K. Morokuma, G.A. Voth, P. Salvador, J.J. Dannenberg, V.G. Zakrzewski, S. Dapprich, A.D. Daniels, M.C. Strain, O. Farkas, D.K. Malick, A.D. Rabuck, K. Raghavachari, J.B. Foresman, J.V. Ortiz, Q. Cui, A.G. Baboul, S. Clifford, J. Cioslowski, B.B. Stefanov, G. Liu, A. Liashenko, P. Piskorz, I. Komaromi, R.L. Martin, D.J. Fox, T. Keith, M.A. Al-Laham, C.Y. Peng, A. Nanayakkara, M. Challacombe, P.M.W. Gill, B. Johnson, W. Chen,

M.W. Wong, C. Gonzalez, J.A. Pople, Gaussian 03, Revision C.02, Gaussian Inc., Pittsburgh, PA, 2003.
[17] W. Kohn, A.D. Becke, R.G. Parr, J. Phys. Chem. 100 (1996) 12974–12980.
[18] A.D. Becke, J. Chem. Phys. 98 (1993) 5648–5652.
[19] C. Lee, W. Yang, R.D. Parr, Phys. Rev. B 37 (1988) 785–789.
[20] G. Psofogiannakis, A. St-Amant, M. Ternan, J. Phys. Chem. B 110 (2006) 24593–24605.
[21] P. Liu, A. Logadottir, J.K. Nørskov, Electrochim. Acta 48 (2003) 3731–3742.
[22] W. Kutzelnigg, Einführung in die Theoretische Chemie, Wiley-VCH, 2002, ISBN 3-527-30609-9.
[23] http://en.wikipedia.org/wiki/Carbon_monoxide.
[24] X. Fang, L. Wang, P.K. Shen, G. Cui, C. Bianchini, J. Power Sources 195 (2010) 1375–1378.
[25] J.S. Spendelow, J.D. Goodpaster, P.J.A. Kenis, A. Wieckowski, Langmuir 22 (2006) 10457–10464.
[26] F. Wen, U. Simon, Chem. Mater. 19 (2007) 3370–3372.